Polaron Effects on the Third-Order Susceptibility of a CdSe/ZnS Quantum Dot Quantum Well

Xi Zhang, Guiguang Xiong, and Xiaobo Feng

Department of Physics, Wuhan University, Wuhan 430072, China

Reprint requests to G. X.; Fax: 86 27 68752569; E-mail:ggxiong@whu.edu.cn

Z. Naturforsch. **64a,** 625 – 631 (2009); received November 18, 2008 / revised February 9, 2009

Theoretical investigation of the polaron effects on the third-order susceptibility associated with the intersubband transition in the conduction band in a CdSe/ZnS quantum dot quantum well is presented. Contributions from the confined longitudinal optical (LO) and surface optical phonon modes are considered and the wave function is derived under the frame work of the perturbation theory. We carried a detailed calculation of third-harmonic generation (THG), Quadratic electro-optic effects (QEOE), and electro-absorption (EA) process on such a quantum dot as a function of pump photon energy with different incident photon energy and under different sizes. The results reveal that the polaron effects are quite important especially around the peak value of the third-order susceptibility. By increasing the size of the quantum dots, the peaks of $\chi^{(3)}_{\mathrm{THG}}$, $\chi^{(3)}_{\mathrm{QEOE}}$, and $\chi^{(3)}_{\mathrm{EA}}$ will shift to the lower energy, and the intensities of the peaks will increase.

Key words: Core-Shell Quantum Dot; Nonlinear Optical Susceptibility; Polarons.
PACS numbers: 73.21.La; 42.65.-k; 74.20.Mn

1. Introduction

In the past decade there has been considerable interest in the nonlinear optical properties of semiconductor quantum dots (QDs) structures, due to their potential applications in optoelectronic and photonic devices [1 – 4]. In these zero-dimensional structures the electron motion is quantized in all three dimensions and this leads to discrete electron energy levels. Because of a δ-like density of states, large optical nonlinearities associated with intersubband transitions occurred in semiconductor quantum dots compared with bulk semiconductor. A great deal of theoretical and experimental work has been done on the study of these zero-dimensional semiconductor systems [5 – 6]. Nowadays, with the development of nano-material fabrication, many methods such as metal-organic chemical vapor deposition (MOCVD), molecular beam epitaxy (MBE), Sol-gel, and molecular imprinted polymer (MIP) are used to synthesize all kinds of quantum dots, including spherical, cylindrical, and pyramidal quantum dots. Among these quantum dots, a synthesized inhomogeneous spherical quantum dot with a core in center and one or several layers of shells called core-shell structure quantum dot or quantum dot quantum well (QDQW), attracts many scientists' interest. CdSe/ZnS quantum dots are one of the most studied quantum dot quantum wells.

It is well known that the electron-optical phonon interaction plays an important part in physical properties of polar crystals, such as the binding energy of impurities, carrier transportation, and linear and nonlinear optical properties [7 – 10]. As we all know, in the low-dimensional quantum systems, phonons are confined. So the phonon modes are more complicated than those in the bulk materials and the bulk phonon modes are no longer suitable [11]. Many researchers have made great contributions in studying the phonon modes and the electron-phonon interaction in low-dimensional semiconductor structures. The electron-phonon interaction in a dielectric confined system was first studied by Lucas et al. [12] and Licari and Evrard [13] under the dielectric continuum model. Wendler and Haupt [14, 15] constructed a complete theory of long-wavelength optical phonons and polar-type electron-phonon interaction for any confined system within the framework of the standard dielectric continuum (DC). The electron-phonon interaction Hamiltonian and the optical-phonon modes in a quantum well were provided by Mori and Ando [16]. Many authors studied polaron effects of QDs. Li and Chen obtained the longitudinal-optical (LO) phonon modes and two

types of surface-optical (SO) phonon mode of a free-standing cylindrical QD [17]. Zhang et al. have derived the Fröhlich electron-phonon interaction Hamiltonian in HgS/CdS quantum dot quantum well (QDQW) [11]. The polaron effects on the third-order nonlinear optical susceptibility in a GaAs quantum disk have been studied by Cui-Hong Liu et al. [18].

There are many analyses about the influence of LO phonon and SO phonon on the energy of an electron in a quantum confined system [8, 9]. The Hamiltonian that describes the coupling of these phonons with electrons and holes was derived by Klein et al. [19]. However, there are few studies treating the electron-phonon interaction on the optical nonlinearities in a core-shell quantum dot. Most researches just focused on a spherical quantum dot that consist of one material. Or they didn't maily investigate the influence of the polaron effect on nonlinear optics. So in this paper, by employing the effective mess approximation methods, we will study the influence of polaron on the third-order nonlinear susceptibilities in a CdSe/ZnS core-shell quantum dot by employing the QDQW phonon modes [11].

2. Theory

2.1. Electron, Phonon and Electron-Phonon Interaction Hamiltonian

We consider an isolated CdSe/ZnS quantum dot quantum well with inner radius R_1 and outer radius R_2 (Fig. 1). Actually, the potential difference of the two materials formed a well and a barrier. The potential in the core is used as the zero reference energy in this paper. The band-gap of the shell layer is wider than that of the core layer, so $V_c > 0$. Under the framework of effective-mass approximation, the Hamiltonian of the system associated with the electron-phonon interaction can be written as

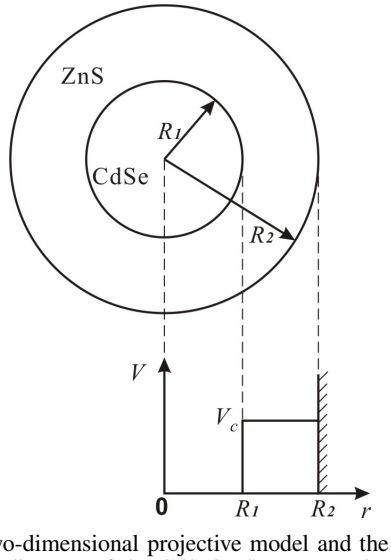

Fig. 1. Two-dimensional projective model and the potential schematic diagram of the CdSe/ZnS quantum dot quantum well.

$$H = H_{\mathrm{e}} + H_{\mathrm{ph}} + H_{\mathrm{e\text{-}ph}}. \tag{1}$$

The first term in (1) is the Hamiltonian of the electron H_{e}, it is given by

$$H_{\mathrm{e}} = -\frac{\hbar^2}{2m_i^*}\nabla^2 + V_i(r), \tag{2}$$

where m_i^* is the effective mass of an electron in the ith region, $V_i(r)$ is the potential. They both depend on the position in the hetero-structure and are expressed as

$$m_i^* = \begin{cases} m_1^*, & r \le R_1 \\ m_2^*, & R_1 < r \le R_2 \end{cases} \tag{3}$$

and

$$V_i(r) = \begin{cases} 0, & 0 < r \le R_1 \\ V_{\mathrm{c}}, & R_1 < r \le R_2 \\ \infty, & r > R_2 \end{cases}. \tag{4}$$

The second term is the free phonon Hamiltonian,

$$\begin{aligned} H_{\mathrm{ph}} &= H_{\mathrm{LO}} + H_{\mathrm{IO,SO}} \\ &= H_{\mathrm{LO1}} + H_{\mathrm{LO2}} + H_{\mathrm{IO,SO}}\,, \end{aligned} \tag{5}$$

where H_{LO1} and H_{LO2} are the Hamiltonian of confined LO phonon modes in the core and in the shell, respectively, $H_{\mathrm{IO,SO}}$ is the Hamiltonian of the interface phonon and surface phonon modes. Using the method in [11], the phonon modes and the Hamiltonian can easily be written as:

$$H_{\mathrm{LO1}} = \sum_{lmn} \hbar\omega_{\mathrm{LO1}} \left[a_{lmn}^{+} a_{lmn} + \frac{1}{2} \right], \tag{6}$$

$$H_{\mathrm{LO2}} = \sum_{lmn} \hbar\omega_{\mathrm{LO2}} \left[b_{lmn}^{+} b_{lmn} + \frac{1}{2} \right], \tag{7}$$

$$H_{\mathrm{IO,SO}} = \sum_{lm} \hbar\omega \left[c_{lm}^{+} c_{lm} + \frac{1}{2} \right], \tag{8}$$

where a^+_{lmn} (a_{lmn}), b^+_{lmn} (b_{lmn}), and c^+_{lm} (c_{lm}) are creation (annihilation) operators for these three phonon modes. They satisfy the commutative rules for bosons. The last term of (1) stands for the electron-phonon interaction Hamiltonian

$$H_{\text{e-ph}} = H_{\text{e-LO1}} + H_{\text{e-LO2}} + H_{\text{e-IO,SO}}. \tag{9}$$

$H_{\text{e-LO1}}$ denotes the Hamiltonian of the electron interaction with LO phonon in the core.

$$H_{\text{e-LO1}} = -\sum_{lmn}\left[\Gamma^{\text{LO1}}_{l,n} j_l\left(\frac{\alpha_{l,n}}{R_1}r\right)Y_{lm}(\theta,\varphi)a^+_{lmn} + H.c.\right], \tag{10}$$

where

$$|\Gamma^{\text{LO1}}_{l,n}|^2 = \frac{4\pi e^2\hbar\omega_{\text{LO1}}}{\alpha^2_{l,n}R_1 j^2_{l+1}(\alpha_{l,n})}\left(\frac{1}{\varepsilon_{1\infty}} - \frac{1}{\varepsilon_{10}}\right). \tag{11}$$

$j_l(x)$ is the spherical Bessel function of the lth order, Y_{lm} is the spherical harmonics, and $\alpha_{l,n}$ is the nth zero of $j_l(x)$. ε_{10}, $\varepsilon_{1\infty}$ are the static and high-frequency dielectric constants in the core layer of the quantum dot, respectively.

Correspondingly, $H_{\text{e-LO2}}$ is the Hamiltonian of the electron interaction with LO phonon in the shell.

$$H_{\text{e-LO2}} = -\sum_{lmn}\left[\Gamma^{\text{LO2}}_{l,n} T_l\left(\frac{a_{l,n}}{R_1}r\right)Y_{lm}(\theta,\varphi)b^+_{lmn} + H.c.\right], \tag{12}$$

with

$$|\Gamma^{\text{LO2}}_{l,n}|^2 = \frac{4\pi e^2\hbar\omega_{\text{LO2}}}{a^2_{l,n}R_1}[T_{l-1}(a_{l,n})T_{l+1}(a_{l,n}) - \gamma^3 T_{l-1}(\gamma a_{l,n})T_{l+1}(\gamma a_{l,n})]^{-1}\left(\frac{1}{\varepsilon_{2\infty}} - \frac{1}{\varepsilon_{20}}\right), \tag{13}$$

where

$$\gamma = R_2/R_1, \tag{14}$$

$$T_l\left(\frac{a_{l,n}}{R_1}r\right) = j_l\left(\frac{a_{l,n}}{R_1}r\right) + b_{l,n}n_l\left(\frac{a_{l,n}}{R_1}r\right). \tag{15}$$

ε_{20}, $\varepsilon_{2\infty}$ are the static and high-frequency dielectric constants in the shell layer of the quantum dot. $n_l(x)$ is the spherical Neumann function of the lth order. $T_l(a_{l,n}r/R_1)$ satisfies the boundary conditions

$$\begin{aligned} T_l\left(\frac{a_{l,n}}{R_1}r\right)\Big|_{r=R_1} &= j_l(a_{l,n}) + b_{l,n}n_l(a_{l,n}) = 0,\\ T_l\left(\frac{a_{l,n}}{R_1}r\right)\Big|_{r=R_2} &= j_l\left(\frac{a_{l,n}}{R_1}R_2\right) + b_{l,n}n_l\left(\frac{a_{l,n}}{R_1}R_2\right) = 0. \end{aligned} \tag{16}$$

From these two equations, $a_{l,n}$ and $b_{l,n}$ can be obtained. n in the radial function $T_l(a_{l,n}r/R_1)$ denotes the number of zeros within the region of $R_1 \le r \le R_2$. In [11], it has been proved that $T_l(a_{l,n}r/R_1)$ is orthogonalized in the shell region.

In (9), the last term $H_{\text{e-IO,SO}}$ is the Hamiltonian of the electron interaction with IO/SO phonon

$$H_{\text{e-IO,SO}} = -\sum_{lm}\Gamma^{\text{IO,SO}}_l(r)[Y_{lm}(\theta,\varphi)c^+_{lm} + H.c.], \tag{17}$$

where the electron-IO or electron-SO phonon radial coupling function is

$$\Gamma^{\text{IO,SO}}_l(r) = N_l \times \begin{cases} \left(\frac{1}{R_2}\gamma^{-l} - \frac{1}{R_1}\gamma^l\right) \text{ for } r \le R_1,\\ \left[\left(\frac{1}{R_2}\gamma^{-l} - \beta^{-l-1}f_l(\omega)\right)r^l + \left(\frac{1}{R_2}\gamma^{-l}f_l(\omega) - \beta^l\right)r^{-l-1}\right]\\ \text{for } R_1 < r \le R_2,\\ \left(\frac{1}{R_2}\gamma^{-l} - \frac{1}{R_1}\gamma^l\right)f_l(\omega)r^{-l-1}\\ \text{for } r > R_2, \end{cases} \tag{18}$$

$$\begin{aligned} |N_l|^2 = 2\pi e^2\hbar\omega\Bigg(&\left(\frac{1}{\varepsilon_1 - \varepsilon_{10}} - \frac{1}{\varepsilon_1 - \varepsilon_{1\infty}}\right)^{-1}\\ &\cdot l(\gamma^{-l-1} - \gamma^l)^2 R_1^{2l-1} + \left\{l\left[\frac{\gamma^{-l}}{R_2} - \beta^{-l-1}f_l(\omega)\right]^2\right.\\ &\cdot(\gamma^{2l+1} - 1)R_1^{2l+1} - (l+1)\left[\frac{1}{R_2}\gamma^{-l}f_l(\omega) - \beta^l\right]^2\\ &\left.\cdot(\gamma^{-2l-1} - 1)R_1^{-2l-1}\right\}\left(\frac{1}{\varepsilon_2 - \varepsilon_{20}} - \frac{1}{\varepsilon_2 - \varepsilon_{2\infty}}\right)^{-1}\Bigg)^{-1}, \end{aligned} \tag{19}$$

where β is defined as

$$\beta = R_1 \cdot R_2. \tag{20}$$

Other than the LO modes, the dielectric functions $\varepsilon_1(\omega)$ and $\varepsilon_2(\omega)$ of the IO or SO phonon don't equal zero. They are given by light scattering topography (LST) relations and written as

$$\begin{aligned} \varepsilon_1(\omega) &= \varepsilon_{1\infty}\frac{\omega^2 - \omega^2_{\text{LO1}}}{\omega^2 - \omega^2_{\text{TO1}}},\\ \varepsilon_2(\omega) &= \varepsilon_{2\infty}\frac{\omega^2 - \omega^2_{\text{LO2}}}{\omega^2 - \omega^2_{\text{TO2}}}. \end{aligned} \tag{21}$$

Together with the boundary conditions [11] at $r = R_1$ and $r = R_2$, the frequencies of the IO and SO

phonons can be derived by solving a sixth-order equation for ω. Once ω is worked out, it is easy to get the values of $\varepsilon_1(\omega)$ and $\varepsilon_2(\omega)$.

And $f_l(\omega)$ reads

$$f_l(\omega) = -\left[\gamma^{-l} l R_2^{l-2}\varepsilon_2 + \beta^l (l+1) R_2^{-l-2}\varepsilon_2\right] / \left[-\beta^{-l-1} l R_2^{l-1}\varepsilon_2 - \gamma^{-l}(l+1)R_2^{-l-3}\varepsilon_2 + (\gamma^{-l} - \gamma^{l+1})(l+1)R_2^{-l-3}\varepsilon_d\right]. \tag{22}$$

2.2. Wave Function and Third-Order Susceptibilities

The wave function and eigenenergy of an electron can be obtained from the Schrödinger equation of an electron when $E_e > V_c$:

$$\Phi^e_{nlm}(r,\theta,\varphi) = R_{nl}(r)Y_{lm}(\theta,\varphi) = \begin{cases} A_1 j_l(k_{nl,1}r)Y_{lm}(\theta,\varphi), \text{ for } r \le R_1, \\ [A_2 j_l(k_{nl,2}r) + B_2 n_l(k_{nl,2}r)]Y_{lm}(\theta,\varphi), \\ \text{for } R_1 < r \le R_2, \end{cases} \tag{23}$$

where n_l is the lth Neumann function. A_1, A_2, and B_2 are normalized constants, and

$$k_{nl,1} = \sqrt{2m_1^* E_e/\hbar^2}, \tag{24}$$

$$k_{nl,2} = \sqrt{2m_2^*(E_e - V_c)/\hbar^2}. \tag{25}$$

At the boundaries $r = R_1$ and $r = R_2$, the continuity of the wave function and the probability current, together with the normalization condition, can give the coefficients A_1, A_2, B_2, and the eigenenergy of the electron E_e.

We limit our consideration to weak coupling and treat the electron-phonon interaction as a perturbation. The unperturbed energy and wave function are turned out to be

$$E_i = E_e^i + \sum_{lmn} N_{lmn}^{LO1}\hbar\omega_{LO1} + \sum_{lmn} N_{lmn}^{LO2}\hbar\omega_{LO2} + \sum_{lm} N_{lm}\hbar\omega_{SO}, \tag{26}$$

$$|\Phi_i\rangle = |n_i, l_i, m_i, N_{lmn}^{LO1}, N_{lmn}^{LO2}, N_{lm}\rangle = \begin{cases} A_1 j_l(k_{nl,1}r)Y_{lm}(\theta,\varphi)|N_{lmn}^{LO1}, N_{lmn}^{LO2}, N_{lm}\rangle, \\ \text{for } r \le R_1, \\ [A_2 j_l(k_{nl,2}r) + B_2 n_l(k_{nl,2}r)] \\ \cdot Y_{lm}(\theta,\varphi)|N_{lmn}^{LO1}, N_{lmn}^{LO2}, N_{lm}\rangle, \\ \text{for } R_1 < r \le R_2, \end{cases} \tag{27}$$

where $|N_{lmn}^{LO1}\rangle$, $|N_{lmn}^{LO2}\rangle$, and $|N_{lm}\rangle$ are the eigenstates of the LO and SO phonon modes in the population presentation. We assumed that the system is at low temperature ($T \to 0$), so the initial state is the phonon vacuum state. Also, in the course of photon transition, only one-phonon absorption (emission) is considered. Under the framework of perturbation theory, the system wave function can be worked out:

$$|\Psi_i\rangle = |\Phi_i\rangle + \sum_{j\ne i} \frac{\lfloor H_{e\text{-}ph}\rfloor_{ji}}{E_i - E_j - \varepsilon}|\Phi_i\rangle, \tag{28}$$

where $\varepsilon = \hbar\omega_{LO}$ or $\hbar\omega_{sp}$.

Using the density matrix method [20, 21], the third-order nonlinear susceptibility tensor is

$$\chi^{(3)}(\omega_p + \omega_q + \omega_r) = \frac{Ne^4}{\varepsilon_0 h^3}\sum_{a,b,c,d}\mu_{ab}\mu_{bc}\mu_{cd}\mu_{da} / [(\omega_{ba}^* - \omega_r - \omega_q - \omega_p)(\omega_{ca}^* - \omega_q - \omega_p)(\omega_{da}^* - \omega_p)] + \frac{\mu_{ab}\mu_{bc}\mu_{cd}\mu_{da}}{(\omega_{ba}^* + \omega_r)(\omega_{ca}^* - \omega_q - \omega_p)(\omega_{da}^* - \omega_p)} + \frac{\mu_{ab}\mu_{bc}\mu_{cd}\mu_{da}}{(\omega_{ba}^* + \omega_r)(\omega_{ca}^* + \omega_q + \omega_p)(\omega_{da}^* - \omega_p)} + \frac{\mu_{ab}\mu_{bc}\mu_{cd}\mu_{da}}{(\omega_{ba}^* + \omega_r)(\omega_{ca}^* + \omega_q + \omega_p)(\omega_{da}^* + \omega_r + \omega_q + \omega_p)}, \tag{29}$$

where $\mu_{ij} = \langle\Psi_i|r|\Psi_j\rangle$, $\omega_{ij} = (E_j - E_i - i\Gamma_{ji})/\hbar$, N is the density of electron in QDs, e the electronic charge, ε_0 the vacuum permittivity, and Γ_{ji} the relaxation rate. Then

$$\mu_{ij} = \langle\Phi_i|r|\Phi_j\rangle + \sum_{\alpha\ne i}^{\infty}\frac{\langle\Phi_\alpha|H_{e\text{-}LO1}|\Phi_i\rangle}{E_i - E_\alpha - \hbar\omega_{LO1}}\langle\Phi_j|r|\Phi_\alpha\rangle + \sum_{\alpha\ne j}^{\infty}\frac{\langle\Phi_\alpha|H_{e\text{-}LO2}|\Phi_j\rangle}{E_j - E_\alpha - \hbar\omega_{LO2}}\langle\Phi_i|r|\Phi_\alpha\rangle + \sum_{\alpha\ne i}^{\infty}\frac{\langle\Phi_\alpha|H_{e\text{-}LO2}|\Phi_i\rangle}{E_i - E_\alpha - \hbar\omega_{LO2}}\langle\Phi_j|r|\Phi_\alpha\rangle + \sum_{\alpha\ne j}^{\infty}\frac{\langle\Phi_\alpha|H_{e\text{-}SO}|\Phi_j\rangle}{E_j - E_\alpha - \hbar\omega_{sp}}\langle\Phi_i|r|\Phi_\alpha\rangle + \sum_{\alpha\ne i}^{\infty}\frac{\langle\Phi_\alpha|H_{e\text{-}SO}|\Phi_i\rangle}{E_i - E_\alpha - \hbar\omega_{sp}}\langle\Phi_j|r|\Phi_\alpha\rangle. \tag{30}$$

In the previous section, the unperturbed wave function, the eigenenergy, and the electron-phonon interaction Hamiltonian have been obtained. Substituting them into (29) and (30), we can get $\chi^{(3)}$.

Table 1. Material parameters (m_0 is the rest electron mass).

Material	m^*/m_0	$\hbar\omega_{\mathrm{LO}}$	ε_0	ε_∞
CdSe [22, 23]	0.13	26 meV	9.56	6.23
ZnS [22, 24]	0.28	43.6 meV	8.1	5.14

3. Results and Discussion

If we assume $\omega_p = \omega_q = \omega_r = \omega$, (29) will give the third-order susceptibility for the third harmonic generation (THG). And if $\omega_p = \omega_q = 0$ and $\omega_r = \omega$, we can obtain the optical susceptibilities $\chi^{(3)}(-\omega;0,0,\omega)$. $\chi^{(3)}_{\mathrm{QEOE}}(\omega) = \mathrm{Re}\chi^{(3)}(-\omega;0,0,\omega)$ and $\chi^{(3)}_{\mathrm{EA}}(\omega) = \mathrm{Im}\chi^{(3)}(-\omega;0,0,\omega)$ are responsible for the direct current (DC) Kerr effect and the electroabsorption process, respectively. In our study, the third-order susceptibilities for THG, QEOE, and EA have been considered.

The analysis of the preceding section is used to calculate several important quantities. For simplicity we will only report the third-order susceptibility of the lowest energy state $l = 0$. In this situation, only the LO phonon mode exist. So we mainly calculate the influence of the LO phonon mode on THG, QEOE, and EA. The parameters of our calculation are listed in Table 1, taking $V_{\mathrm{c}} = 0.9$ eV as conduction band discontinuity, electron density $N = 5 \times 10^{24}$ m^{-3}, and $\Gamma_{ji} = 1/300$ fs^{-1}.

In Figure 2, we plotted the third-order susceptibility $\chi^{(3)}$ for the three nonlinear optical effects THG (a), QEOE (b), and EA (c) as a function of pump photon energy $\hbar\omega$. The size of the quantum dot is chosen as $R_1 = 4.5$ nm and $R_2 = 6$ nm. It is seen from Figure 2 that for a CdSe/ZnS quantum dot quantum well the resonant $\chi^{(3)}$ magnitudes are 10^{-16} m^2/V^2. The curves in Figure 2a have three peaks while those in Figure 2b and c only show one peak. As seen from (29), the condition of triple resonance is satisfied for QEOE and EA, whereas only single resonance occurs for THG. The contributions of the LO phonon modes to the polaron effects on third-order susceptibility are demonstrated in Figure 2. It is clearly seen that the LO phonon modes enhance $\chi^{(3)}$, especially around the peak value. This is due to the increment of the dipolar matrix element when considering the contributions of the electron-phonon interaction. A very interesting feature in Figure 2b and c is that near the resonant frequency, $\chi^{(3)}_{\mathrm{QEOE}}(\omega)$ changes its sign from negative to positive while $\chi^{(3)}_{\mathrm{EA}}(\omega)$ always keeps negative. Increasing the frequency slightly, $\chi^{(3)}_{\mathrm{EA}}(\omega)$ fast reaches

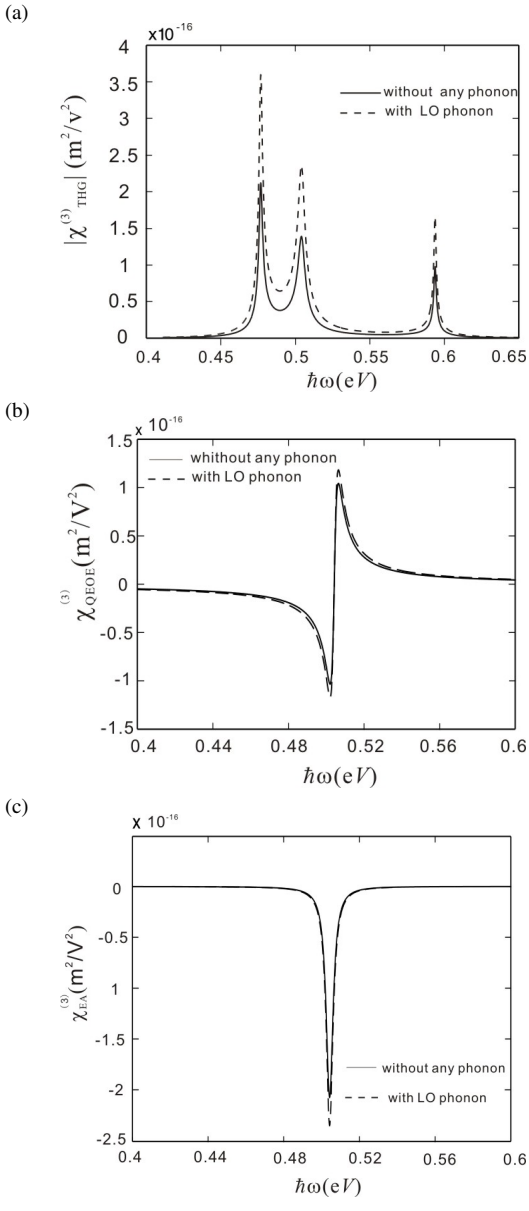

Fig. 2. Contributions of LO phonon modes to (a) THG, (b) QEOE, (c) EA as a function of the photon energy for the CdSe/ZnS quantum dot quantum well ($R_1 = 4.5$ nm, $R_2 = 6$ nm).

a negative maximum. This is important for the further development of quantum dots for optical nonlinear devices.

In Figure 3 $\chi^{(3)}_{\mathrm{THG}}$ (a), $\chi^{(3)}_{\mathrm{QEOE}}$ (b), and $\chi^{(3)}_{\mathrm{EA}}$ (c) are shown as functions of pump photon energy $\hbar\omega$ for different outer radii R_2 (4.8 nm, 5 nm, 5.2 nm) with a fixed inner radius R_1 (4.5 nm). We can find that the

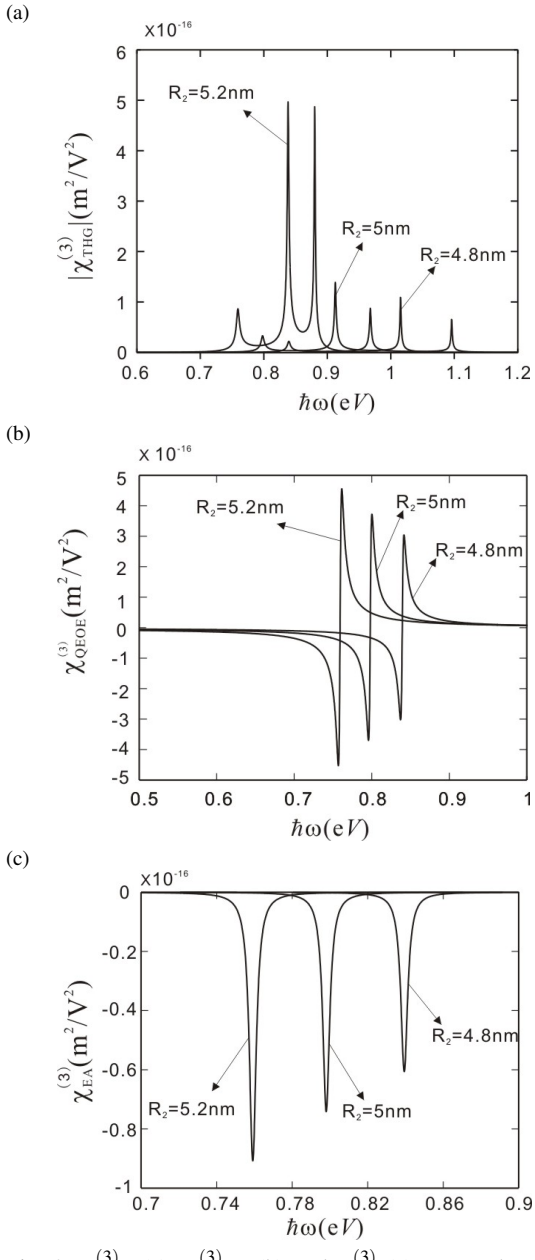

Fig. 3. $\chi^{(3)}_{\mathrm{THG}}$ (a), $\chi^{(3)}_{\mathrm{QEOE}}$ (b) and $\chi^{(3)}_{\mathrm{EA}}$ (c) versus the pump photon energy $\hbar\omega$ with fixed $R_1 = 4.5$ nm.

nonlinear susceptibilities increase and the peaks shift to lower energy as R_2 increases. These conclusions can be physically explained as follows [25]: as a consequence of the quantum size effect, energy distances between electronic states in the conduction band become smaller when R increases; the larger the size, the smaller the energy distance; and the larger the size, the stronger the electron-phonon interactions; the increase of the dipole matrix element μ becomes stronger with the increase of the radius.

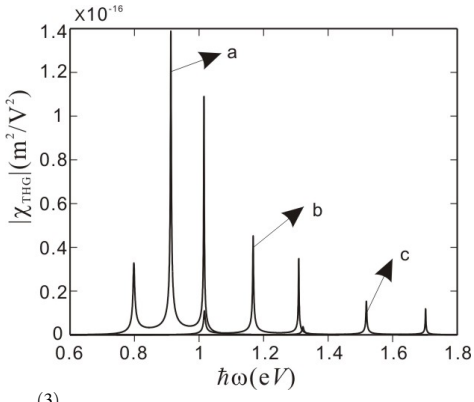

Fig. 4. $\chi^{(3)}_{\mathrm{THG}}$ versus the pump photon energy $\hbar\omega$ with fixed thickness ratio $k = 1/10$; (a): $R_1 = 4.5$ nm, $R_2 = 4.95$ nm; (b): $R_1 = 4$ nm, $R_2 = 4.4$ nm; (c): $R_1 = 3.5$ nm, $R_2 = 3.85$ nm.

Figure 4 is a plot of $\chi^{(3)}_{\mathrm{THG}}$ versus pump photon energy $\hbar\omega$ for different outer radii R_2 and inner radii R_1 with a fixed thickness ratio k, $k = (R_2 - R_1)/R_1$. In Figure 4, we chose $k = 1/10$. We can find that it is similar to Figure 3a, under a fixed thickness ration the $\chi^{(3)}_{\mathrm{THG}}$ enhances with the increase of quantum dot's size. So in order to obtain a large nonlinear susceptibility, we should choose quantum dots with bigger radii. Of course, if the radii of the quantum dots are beyond the scale of nanostructure, the principle of the quantum theory is unavailable and the optical properties of the dots belong to the region of bulk materials.

4. Conclusion

In conclusion, the polaron effects on the nonlinear optical susceptibility have been investigated theoretically. Numerical calculations to study the third-order nonlinear optical susceptibilities of CdSe/ZnS quantum dot quantum well by considering the influences of electron-LO phonon interactions have been performed in this paper. We have obtained the size dependent third-order nonlinear optical susceptibilities for THG, QEOE, and EA under strong confinement. The results reveal that LO phonons enhance $\chi^{(3)}$ especially around the peak value. So it is necessary to consider the contributions of the interaction of the electron-phonon. When the sizes of the quantum dots are increased the peaks of $\chi^{(3)}_{\mathrm{THG}}$, $\chi^{(3)}_{\mathrm{QEOE}}$, and $\chi^{(3)}_{\mathrm{EA}}$ as a function of pump photon energy $\hbar\omega$ have a red shift, and the intensities of the peaks increase.

Our numerical calculations don't take into account the influence of the SO phonon. Further work can be done to consider this. Besides, if the potential is changed to be parabolic, just like the study work on quantum wells [26], the sensitivity of the results with respect to variations in the potential can be studied, which may be done in future.

Acknowledgments

This work was financially supported by the National Natral Foundation of China under Grant No. 10534030.

[1] S. Yano, T. Goto, T. Itoh, and A. Kasuya, Phys. Rev. B **55**, 1667 (1997).
[2] T. Akiyama, O. Wada, H. Kuwatsuka, T. Simoyama, Y. Nakata, K. Mukai, M. Sugawara, and H. Ishikawa, Appl. Phys. Lett. **77**, 1753 (2000).
[3] S. A. Podoshvedov, Optics Communication **189**, 365 (2001).
[4] M. Sheik-Bahae, J. Wang, R. Desalvo, D. J. Hagan, and E. W. Van Stryland, Opt. Lett. **17**, 258 (1992).
[5] K. X. Guo, Solid State Commun. **103**, 255 (1997).
[6] S. V. Nair and T. Takagahara, Phys. Rev. B **55**, 5153 (1997).
[7] C. Chuan-Yu, L. Wangsang, and J. Pei-Wan, Commu. Theor. Phys. **28**, 9 (1997).
[8] H.-J. Xie, C.-Y. Chen, and B.-K. Ma, J. Phys: Condens. Matter. **12**, 8623 (2000).
[9] H.-J. Xie, C.-Y. Chen, and B.-K. Ma, Phys. Rev. B **61**, 4827 (2000).
[10] H.-J. Xie and C.-Y. Chen, Eur. Phys. J. B **5**, 215 (1998).
[11] L. Zhang, H.-J. Xie, and C.-Y. Chen, Phys. Rev. B **66**, 205326 (2002).
[12] A. A. Lucas, E. Kartheuser, and R. G. Bardro, Phys. Rev. B **41**, 1439 (1970).
[13] J. J. Licari and R. Evrard, Phys. Rev. B **15**, 2254 (1977).
[14] L. Wendler, Phys. Status Solidi B **129**, 513 (1985).
[15] L. Wendler and R. Haupt, Phys. Status Solidi B **143**, 487 (1985).
[16] N. Mori and T. Ando, Phys. Rev. B **40**, 6175 (1989).
[17] W.-S. Li and C.-Y. Chen, Physica B **229**, 375 (1997)
[18] C.-H. Liu, K.-X. Gua, C.-Y. Chen, and B.-K. Ma, Physica E **15**, 217 (2002).
[19] M. C. Klein, F. Hache, D. Ricard, and C. Flytzanis, Phys. Rev. B **42**, 11123 (1990).
[20] T. Takagahara, Phys. Rev. B **39**, 10206. (1989).
[21] E. Rosencher and P. Bois, Phys. Rev. B **44**, 11315 (1991).
[22] J. W. Haus, H. S. Zhou, I. Honma, and H. Komiyama, Phys. Rev. B **47**, 1359 (1993).
[23] A. M. Alcalde and G. E. Marques, Phys. Rev. B **65**, 113301 (2002).
[24] M. A. Kanehisa, D. Petritis, and M. Balkanski, Phys. Rev. B **31**, 6469 (1985).
[25] L. Liu, J. Li, and G. Xiong, Physica E **25**, 466 (2005).
[26] C.-J. Zhang and K.-X. Guo, Physica E **39**, 103 (2007).